Doping Effect on High-Pressure Structural Stability of ZnO Nanowires

ARTICLE *in* THE JOURNAL OF PHYSICAL CHEMISTRY C · DECEMBER 2008

Impact Factor: 4.77 · DOI: 10.1021/jp809919a

8 AUTHORS, INCLUDING:

Gu Yousong
University of Science and Technology Beijing
86 PUBLICATIONS **671** CITATIONS
SEE PROFILE

Yunhua Huang
University of Science and Technology Beijing
83 PUBLICATIONS **1,045** CITATIONS
SEE PROFILE

Yue Zhang
Fudan University
334 PUBLICATIONS **3,583** CITATIONS
SEE PROFILE

THE JOURNAL OF PHYSICAL CHEMISTRY C

Letter

Doping Effect on High-Pressure Structural Stability of ZnO Nanowires

Xiaoqin Yan, Yousong Gu, Xiaomei Zhang, Yunhua Huang,
Junjie Qi, Yue Zhang, Takeshi Fujita, and Mingwei Chen

J. Phys. Chem. C, **2009**, 113 (4), 1164-1167• DOI: 10.1021/jp809919a • Publication Date (Web): 31 December 2008

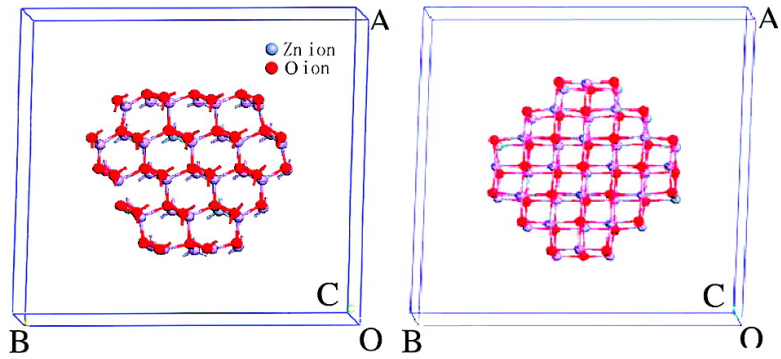

More About This Article

Additional resources and features associated with this article are available within the HTML version:

- Supporting Information
- Access to high resolution figures
- Links to articles and content related to this article
- Copyright permission to reproduce figures and/or text from this article

View the Full Text HTML

THE JOURNAL OF PHYSICAL CHEMISTRY C LETTERS

2009, *113,* 1164–1167
Published on Web 12/31/2008

Doping Effect on High-Pressure Structural Stability of ZnO Nanowires

Xiaoqin Yan,[†] Yousong Gu,[†] Xiaomei Zhang,[†] Yunhua Huang,[†] Junjie Qi,[†] Yue Zhang,*[,†,‡] Takeshi Fujita,[§] and Mingwei Chen*[,§]

Department of Materials Physics and Chemistry, University of Science & Technology Beijing, Beijing 100083, China, State Key Laboratory for Advanced Metals and Materials, University of Science & Technology Beijing, Beijing 100083, China, and World Premier International Research Center, Advanced Institute for Materials Research, Tohoku University, Sendai 980-8577, Japan

Received: November 11, 2008; Revised Manuscript Received: December 11, 2008

We report reversible phase transitions of ZnO nanowires subjected to high-pressure diamond anvil cell experiments. It was found that Mn doping obviously changes the elastic stability of ZnO nanowires and leads to low critical pressures of the reversible transitions between wurtzite to rocksalt phases during compression and decompression. First-principles calculations demonstrate that the lower critical pressures caused by Mn doping are associated with the decrease of internal energy difference and the increase of relative volume change between wurtzite to rocksalt phases.

Introduction

Nanostructured ZnO has potential applications in electronics, optoelectronics, photovoltaics, and sensors.[1−3] At ambient conditions, ZnO has a hexagonal wurtzite (B_4) structure (space group $P6_3mc$), in which the Zn (or O) atoms are tetrahedrally coordinated to four O (or Zn) atoms. At a high pressure above 9.0 GPa, a phase transition from B4 to cubic rocksalt (B1) structure (space group $Fm\bar{3}m$) occurs with an increased coordination number from 4 to 6.[4] This high-pressure phase transition has been widely investigated by energy dispersive X-ray diffraction,[5−7] X-ray-absorption near-edge structure,[8] Raman scattering,[9] and photoluminescence measurements.[10] Recently, the high-pressure transition from wurtzite to rocksalt phases (W-to-R) has also been observed in ZnO nanoparticles.[11] Practically, in order to combine semiconductivity and ferromagnetism into existing semiconductor devices for the applications of nonvolatile memory and quantum computation,[12,13] ZnO was frequently doped with transition metals (e.g., Mn, Co, Fe, Cu, and Ni). Metal-doped ZnO nanowires and nanoparticles have been fabricated successfully, which are a promising candidate for a transparent diluted magnetic semiconductor in spintronics.[14−16] However, the doping effects on the high-pressure structural stability of nanostructured ZnO have not been fully understood. In this study, we systematically investigated high-pressure phase transitions in pure and Mn-doped ZnO nanowires by in situ high-pressure Raman spectroscopy and first-principles simulations.

Experimental Section

Pure and doped ZnO nanowires were synthesized by a vapor phase deposition method.[17] The products were examined by a field-emission scanning electron microscope (SEM; Philips XL 30 FEG) and a transmission electron microscope (TEM; JEM-2010F at 200kv) equipped with an energy-dispersive X-ray (EDX) spectrometer. X-ray diffraction data of the samples were collected using RINT-2200 Ultima-III diffractometer with a rotating anode Cu radiation operated at 40 kV and 40 mA. The scanning angle (2θ) ranges from 20 to 80° at a step of 0.01°.

A piston-cylinder type diamond anvil cell (DAC) combined with micro-Raman spectroscopy was employed to investigate high-pressure phase transitions of single-crystal ZnO nanowires with and without Mn doping. A 16:3:1 methanol:ethanol:water solution was used as the pressure-transmitting medium. The applied pressures were measured by both the ruby luminescence[18] and diamond Raman scales.[19] A micro-Raman spectrometer (Renishaw, UK) with an Ar^+ laser (514.5 nm) was employed to characterize the structure changes of ZnO nanowiers caused by high pressures at room temperature.

Results and Discussion

Figure 1a shows that nanowires are randomly distributed on a Si substrate. The nanowires have a diameter ranging from ∼60 to 100 nm and length of about tens of microns. The microstructure and composition of the nanowires were further characterized by TEM in details. Bright-field TEM observations demonstrate that individual nanowires are a single crystal without detectable grain boundaries [Figure 1b]. The corresponding EDX spectrum of the Mn doped nanowires reveals that the nanowires are composed of Zn, O and Mn, and the concentration of Mn is about 4.84 at.% [Figure 1c]. XRD measurements were made on the mass of nanowires to assess the overall structure and phase purity. The typical XRD patterns taken from the pure and Mn-doped ZnO nanowires were shown in Figure 1d. All of the diffraction peaks of the pure ZnO nanowires can be indexed to the known wurtzite structure of ZnO with lattice constants of $a = 0.3247$ nm and $c = 0.5201$ nm. For the Mn-doped ZnO nanowires, a new phase or impurity

* To whom correspondence should be addressed. E-mail: yuezhang@ustb.edu.cn; mwchen@imr.tohoku.ac.jp.
[†] Department of Materials Physics and Chemistry, University of Science & Technology Beijing.
[‡] State Key Laboratory for Advanced Metals and Materials, University of Science & Technology Beijing.
[§] Tohoku University.

10.1021/jp809919a CCC: $40.75

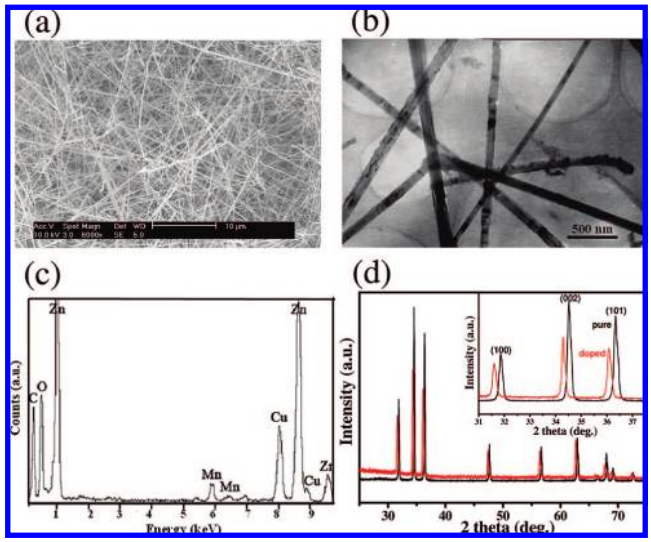

Figure 1. (a) SEM image of Mn-doped ZnO nanowires on a Si substrate; (b) TEM micrograph of Mn-doped ZnO nanowires; (c) EDX spectrum of Mn-doped ZnO nanowires; and (d) XRD patterns taken from pure and Mn-doped ZnO nanowires.

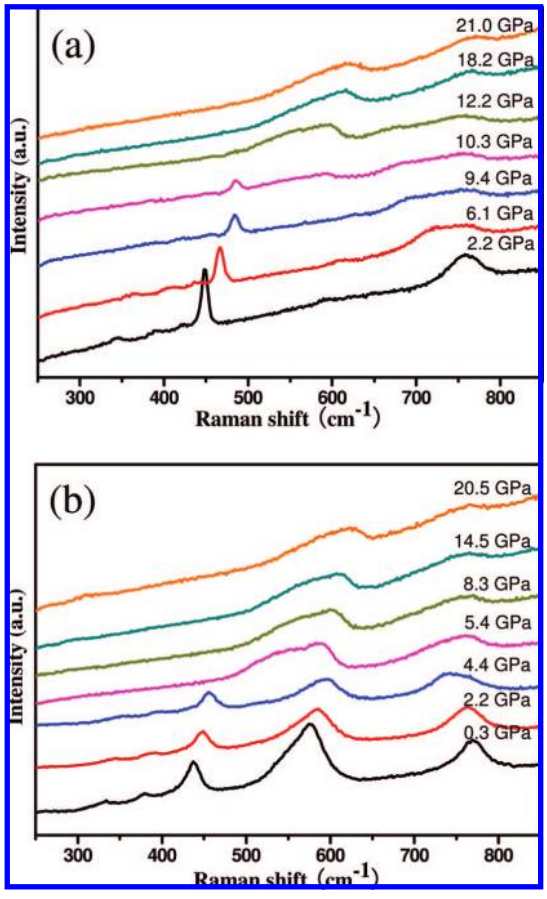

Figure 2. High-pressure Raman spectra of pure ZnO nanowires loaded in DAC. (a) Raman spectra of pure ZnO nanowires loaded from ambient up to 21.0 GPa. The Raman peaks with wurtzite structure disappear at the pressures of above ~10.3 GPa. (b) Raman spectra of pure ZnO nanowires with decompressed pressures from 20.5 to ~0.3 GPa. Reversible wurtzite phase with a characteristic Raman mode E_2^{high} emerges when the pressures is below ~4.4 GPa.

phase has not been detected. However, the diffraction peaks of the Mn-doped ZnO shift to lower 2θ angle in comparison with those of the pure ZnO, which agrees well with the fact that Mn^{2+} ion (0.091 nm) has a larger size than Zn^{2+} ion (0.083 nm). The measured lattice parameters of the Mn doped ZnO nanowires are $a = 0.3263$ nm and $c = 0.5222$ nm, about 0.4~0.5% larger than those of pure ZnO wires, which is consistent with previous report in Mn-doped ZnO films.[20]

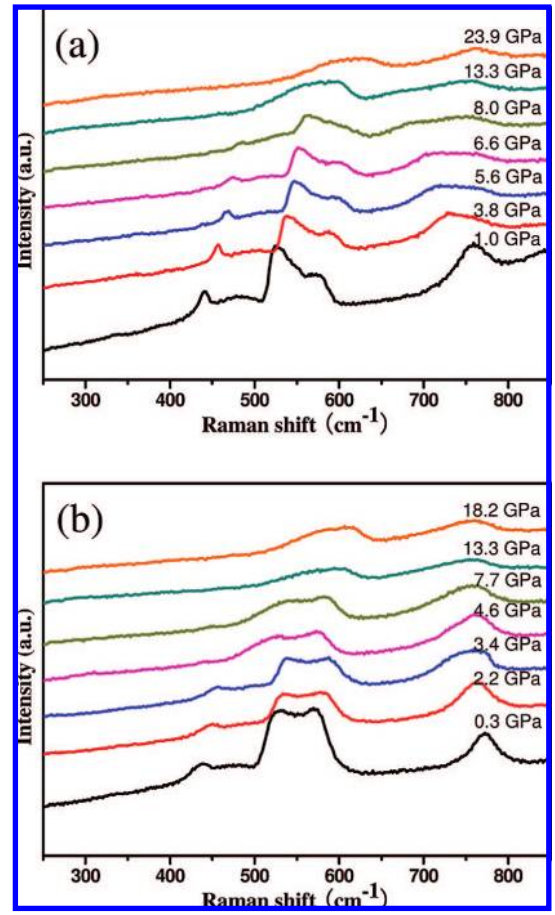

Figure 3. High-pressure Raman spectra of Mn-doped ZnO nanowires loaded in DAC. (a) Raman spectra of ZnO nanowires with Mn doping pressurized from ambient up to 23.9 GPa. The W-R phase transition occurs at the pressures of above ~8.0 GPa. (b) Raman spectra of Mn-doped ZnO nanowires depressurized from 18.2 to ~0.3 GPa. Reversible wurtzite phase emerges at the pressures below ~3.4 GPa.

In this study, DAC combined with micro-Raman spectroscopy was employed to investigate high-pressure phase transitions of pure and Mn-doped single-crystal ZnO nanowires. Figure 2a shows in situ Raman spectra of pure ZnO nanowires at various loading pressures. From low-pressure spectra (for an example, the one at ~2.2 GPa), all Raman active modes of crystalline ZnO can be observed, including the $E_2^{high} - E_2^{low}$, $A_1(TO)$, $E_1(TO)$, E_2^{high}, and $A_1(LO)$ modes.[21] The Raman peak at about 750 cm^{-1} is attributed to the 'half-frequency' of diamond Raman line at 1332 cm^{-1}. With the increase of applied pressures up to 10.3 GPa, the characteristic E_2^{high} mode shifts to higher frequencies and the $A_1(LO)$ becomes very weak. When the applied pressure is above 10.3 GPa, all Raman peaks of wurtzite ZnO disappear due to the W-to-R structural transformation, which is in agreement with the previous high-pressure observations.[9] Meanwhile, a new broad peak at about 600 cm^{-1} appears, which is associated with intrinsic lattice defects caused by the W-to-R phase transition at high pressures.[22] To detect possible phase transitions during depressurization, in situ Raman characterization was performed when the applied pressure was gradually decreased from 21.0 to ~0.3 GPa [Figure 2b]. Accompanying the depressurization, the peak shift of the ZnO Raman bands takes place along the directions opposite to those during

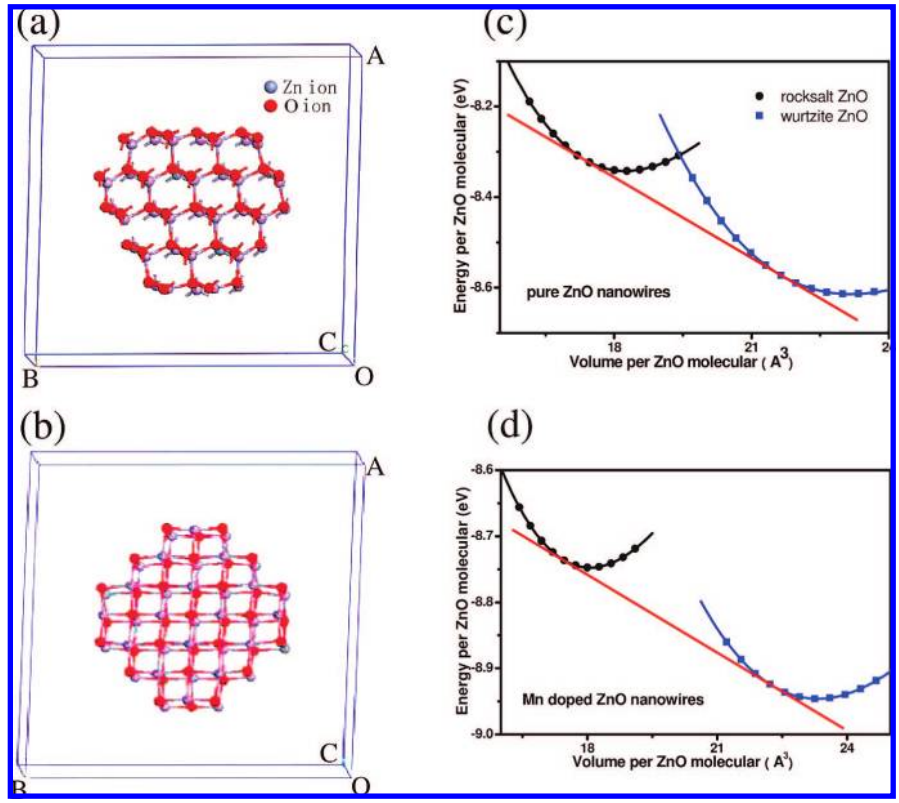

Figure 4. (a and b) The unit cells of wurtzite and rocksalt structures of ZnO Nanowires and (c and d) first-principles calculations on phase transitions of pure and Mn-doped ZnO nanowires.

pressurizing, i.e., E_2^{high} and A_1(LO) modes downshift to 437 and 576 cm^{-1} at the ambient pressure, respectively. Interestingly, a reversible phase transition takes place during the unloading. The characteristic Raman bands of the wurtzite phase appear again when the pressures are below ~4.4 GPa.

Figure 3, panels a and b, shows Raman spectra of Mn-doped ZnO nanowires pressurized up to ~23.9 GPa and depressurized to ~0.3 GPa. In the spectra of Mn-doped ZnO, there is an additional Raman peak at 527 cm^{-1}, corresponding to Mn dopant.[23] Similar to the pure ZnO nanowires, the reversible phase transitions between W-to-R phases can be observed during compression and decompression. However, the critical pressures are much lower for both pressurization and depressurization phase transitions in comparison with those of the pure ones. During pressurization, the wurtzite structure of the doped samples disappears at the pressure of ~8.0 GPa, which is ~2 GPa lower than that of pure ZnO nanowires. For the depressurization transition, the critical pressure of the doped sample is ~3.4 GPa, which is ~1 GPa lower than that of the pure ZnO nanowires. Therefore, manganese doping promotes the high-pressure phase transitions of ZnO nanowires.

Structural transformations of ZnO nanowires subjected to high pressures were also investigated by the first-principles calculations in the framework of density functional theory with pseudopotential and plane-wave basis sets.[24−26] In order to deal with the strong correlation of the d electrons, L(S) DA+U types on site self-interaction were taken into account, and the U value is assumed to be 7.0 eV for Zn, which is based both on literatures and our experiences in bulk ZnO band structure calculation.[27] The energy cutoff was 600 eV for good convergence during geometry optimization. Monkhorst type of k points meshes were generated automatically with a linear density of 40 per $Å^{-1}$. Full geometry relaxations are performed in the case of equilibrium volume, and a uniform scale factor is applied to the lattice constants to calculate the ground-state energies at various volumes. Here isotropic elastic constants are assumed in our calculation. The critical transition pressures are evaluated from the energy versus volume curves. The slope of the common tangent of the energy−volume curves of the W and R phases is used to estimate the transition pressures because the free enthalpy $H = U + PV$ determines the stable phase in a constant pressure environment. Considering the case of nanowires, periodically distributed nanowire arrays were used for the calculations. The distances between the nanowires are larger than 10 Å to eliminate the interactions between the adjacent nanowires. In this case, the unit cell used in calculations is a react angle box with a section of nanowire in the center. In the axial direction, the periodicity is the same as bulk ZnO, whereas in the cross section, the periodicity is the same as the arrangement of the nanowire arrays. The unit cells with 74 atoms of wurtzite structure and rocksalt structure of pure ZnO Nanowires [Figure 4, panels a and b] are used to calculate phase transition. For the Mn doped ZnO nanowires, two Zn ions in a unit cell are replaced by two Mn ions. In our calculations, ferromagnetic coupling is assumed based on the experimental results that Mn doped ZnO nanowires are ferromagnetic.[28] There

TABLE 1: Calculated Results of Phase Transition from Wurtzite to Rocksalt in Pure and Mn-Doped ZnO Nanowires[a]

nanowire	U_w	V_w	U_r	V_r	ΔU	$\Delta V/V_w$	P_{tr}
pure	−8.572	21.632	−8.316	17.320	−0.256	0.199	9.499
Mn-doped	−8.925	22.245	−8.736	17.448	−0.189	0.216	6.304

[a] U denotes the energy (unit eV) and V denotes the volume at transition point (unit $Å^3$). $\Delta V/V_w$ is the relative change of volume from wurtzite to rocksalt structure, where Vw is the volume of wurtzite ZnO. P_{tr} denotes the transition pressure (unit GPa) corresponding to the onset of the phase transition.

are too many doping configurations than we can possibly calculate due to our limited computation power. Thus, we only select several symmetric doping configurations with Mn ions at various distances from the center and choose the equilibrium configurations with the lowest ground states energy to perform the E ~ V calculation. It is found that configuration with Mn ions at modest distance is preferred. Figure 4, panels c and d, presents the calculated curves of the energy per ZnO molecular versus the volume per ZnO molecular for pure and Mn-doped ZnO nanowires. The common tangent to the curves indicates the transition pressures (P_{tr}) from W to R structure of the doped and undoped ZnO nanowires. The calculated results, including the difference of internal energy (ΔU), relative volume changes ($\Delta V/V_w$), and transition pressure (P_{tr}), are listed in Table 1. For the pure ZnO nanowires, the transition pressure from W to R phases is about 9.499 GPa with a relative volume change of 19.9%, whereas for Mn-doped ZnO nanowires the calculated transition pressure is about 6.304 GPa with ($\Delta V/V_w$) = 21.6%. The transition pressure decreases with the Mn doping, which is fairly consistent with the in situ high-pressure Raman observations. The first-principles calculations also reveal that the doping effect on the reduced transition pressures results from the decrease of internal energy difference (ΔU) between the W and R phases and the increase of relative volume changes ($\Delta V/V_w$) from W to R phase after Mn doping.

Conclusions

In summary, the phase transitions of pure and Mn-doped ZnO nanowires were investigated by in situ high pressure Raman spectroscopy. It was found that Mn doping significantly promotes the high-pressure phase transitions of ZnO nanowires at much low pressures. The first-principles calculations suggest that the doping effect is associated with the decrease of internal energy difference and the increase of relative volume change between W and R phases.

Acknowledgment. We acknowledge the financial support from National Basic Research Program of China (No. 2007CB936201), the National High Technology Research and Development Program of China (No. 2006AA03Z351), and the Major Project of International Cooperation and Exchanges (No. 50620120439 and 2006DFB51000). T.F. and M.W.C. are thankful for the support of the "Grant-in-Aid Wakate B", JSPS, and "Global COE for Materials Research and Education" MEXT, Japan.

References and Notes

(1) Minne, S. C.; Manalis, S. R.; Quate, C. F. *Appl. Phys. Lett.* **1995**, *67*, 3918.
(2) Gorla, C. R.; Emanetoglu, N. W.; Liang, S.; Mayo, W. E.; Lu, Y.; Wraback, M.; Shen, H. J. *Appl. Phys. Lett.* **1999**, *85*, 2595.
(3) Huang, Y. H.; Zhang, Y.; Gu, Y. S.; Bai, X. D.; Qi, J. J.; Liao, Q. L.; Liu, J. *J. Phys. Chem. C* **2007**, *111*, 9039.
(4) Bates, C. H.; White, W. B.; Roy, R. *Science* **1962**, *137*, 993.
(5) Desgrenier, S. *Phys. Rev. B* **1998**, *58*, 14102.
(6) Liu, H. Z.; Ding, Y.; Somayazulu, M.; Qian, J.; Shu, J. F.; Häusermann, D.; Mao, H. K. *Phys. Rev. B* **2005**, *71*, 212103.
(7) Liu, H. Z.; Tse, J. S.; Mao, H. K. *J. Appl. Phys.* **2006**, *100*, 093509.
(8) Decremps, F.; Datchi, F.; Saitta, A. M.; Polian, A.; Pascarelli, S.; Di Cicco, A.; Itié, J. P.; Baudelet, F. *Phys. Rev. B* **2003**, *68*, 104101.
(9) Decremps, F.; Pellicer-Porres, J.; Marco Saitta, A.; Chervin, J.-C.; Polian, A. *Phys. Rev. B* **2002**, *65*, 092101.
(10) Shan, W.; Walukiewicz, W.; Ager, J. W., III; Yu, K. M.; Zhang, Y.; Mao, S. S.; Kling, R.; Kirchner, C.; Waag, A. *Appl. Phys. Lett.* **2005**, *86*, 153117.
(11) Kumar, R. S.; Cornelius, A. L.; Nicol, M. F. *Curr. Appl. Phys.* **2007**, *7*, 135.
(12) Ohno, H. *Science* **1998**, *281*, 951.
(13) Wolf, S. A.; Awschalom, D. D.; Buhrman, R. A.; Daughton, J. M.; von Molnár, S.; Roukes, M. L.; Chtchelkanova, A. Y.; Treger, D. M. *Science* **2001**, *294*, 1488.
(14) Norton, D. P.; Pearton, S. J.; Hebard, A. F.; Theodoropoulou, N.; Boatner, L. A.; Wilson, R. G. *Appl. Phys. Lett.* **2003**, *82*, 239.
(15) Spaldin, N. A. *Phys. Rev. B* **2004**, *69*, 125201.
(16) Gratens, X.; Bindilatti, V.; Oliveira, N. F.; Shapira, Y.; Foner, S.; Golacki, Z.; Haas, T. E. *Phys. Rev. B* **2004**, *69*, 125209.
(17) Zhang, X. M.; Zhang, Y.; Wang, Z. L.; Mai, W. J.; Gu, Y. D.; Chu, W. S.; Wu, Z. Y. *Appl. Phys. Lett.* **2008**, *92*, 162102.
(18) Mao, H. K.; Bell, P. M.; Shaner, J. W.; Steinberg, D. J. *J. Appl. Phys.* **1978**, *49*, 3276.
(19) Kresse, G.; Furthmuller, J. *Phys. Rev. B* **1996**, *54*, 11169.
(20) Tiwari, A.; Jin, C.; Kvit, A.; Kumar, D.; Muth, J. F.; Narayan, J. *Solid State Commun.* **2002**, *121*, 371.
(21) Calleja, J. M.; Cardona, M. *Phys. Rev. B* **1977**, *16*, 3753.
(22) Cuscó, R.; Alarcón-Lladó, E.; Ibáñez, J.; Artús, L.; Jiménez, J.; Wang, B. G.; Callahan, M. J. *Phys. Rev. B* **2007**, *75*, 165202.
(23) Du, C. L.; Gu, Z. B.; Lu, M. H.; Wang, J.; Zhang, S. T.; Zhao, J.; Cheng, G. X.; Heng, H.; Chen, Y. F. *J. Appl. Phys.* **2006**, *99*, 123515.
(24) Hanfland, M.; Syassen, K. *J. Appl. Phys.* **1985**, *57*, 2752.
(25) Kohn, W; Sham, L. J. *Phys. Rev.* **1965**, *140*, 1133.
(26) Car, R.; Parrinello, M. *Phys. Rev. Lett.* **1985**, *55*, 2471.
(27) Dong, C. L.; Persson, C.; Vayssieres, L.; Augustsson, A.; Schmitt, T.; Mattesini, M.; Ahuja, R.; Chang, C. L.; Guo, J. H. *Phys. Rev. B* **2004**, *70*, 195325.
(28) Liu, J. J.; Wang, K.; Yu, M. H.; Zhou, W. L. *J. Appl. Phys.* **2007**, *102*, 024301.

JP809919A